JOURNAL OF SPACECRAFT AND ROCKETS
Vol. 31, No. 3, May–June 1994

Development of an Efficient Inverse Method for Supersonic and Hypersonic Body Design

Jaewoo Lee* and W. H. Mason†
Virginia Polytechnic Institute and State University, Blacksburg, Virginia 24061

An efficient inverse method for supersonic and moderate hypersonic axisymmetric body design is developed for the Euler equations. Numerous surface pressure-body geometry rules are examined to obtain an inverse procedure that is robust, yet demonstrates fast convergence. Each rule is analyzed and examined numerically within the inverse calculation routine for supersonic ($M_\infty = 3.0$) and moderate hypersonic ($M_\infty = 6.28$) speeds. Based on the analysis, a new method to obtain rapid, reliable convergence is presented. Example results are given for several demanding cases: a hypersonic minimum drag body and several bodies derived from specification of extreme target pressure distributions. The new method requires slightly more than twice the CPU time of a direct calculation.

Nomenclature

$A(M_L, \theta)$	= constant of proportionality in surface pressure - body shape rule, Eqs. (11–16)
C_p	= pressure coefficient
C_p^T	= surface target pressure coefficient
C_{pvac}	= vacuum pressure coefficient
c	= $(5\gamma M_L^{3/2})^{-1}$
i	= marching plane index
k	= the inverse iteration count
k_l	= hypersonic similarity parameter, $M_\infty\theta$, Eq. (7)
M_∞	= freestream Mach number
M_L	= local Mach number at the body surface
P_i	= surface pressure at the marching plane i
r	= body radius
x, y, z	= physical coordinates
γ	= ratio of specific heats
δ	= convergence criterion for the inverse calculation
θ	= body slope angle
τ	= constant, Eq. (8)

Introduction

RENEWED interest in supersonic High Speed Civil Transport (HSCT) and hypersonic National Aerospace Plane (NASP) flight vehicles is leading to requirements for practical aerodynamic design methods for these speed regimes.[1] In particular, the Douglas Aircraft study[2] of supersonic cruise airplanes identified the need for an inverse method that will allow the aerodynamic designer to specify a pressure distribution consistent with the requirements for maintaining laminar flow. Candidate aerodynamic design methods are generally divided into two categories: inverse methods and numerical optimization using direct analysis methods repetitively. The two approaches each have strengths and weaknesses and are perhaps best if used together for current design projects. In particular, inverse methods can be used to generate the design variables or "shape functions" required for numerical optimization. This approach is part of the "Smart Aerodynamic Optimization" concept described in Ref. 3.

The possibility of employing numerical optimization methods arose only after significant computer power became generally available. Thus these methods are the most recent, most expensive, and possibly the most promising ones in the long run. Perhaps the key advantage is the prospect of finding an optimal body shape directly. However, these methods depend critically on the user assumed form of the answer (both in selecting the design variables and the objective function), and, moreover, local rather than global optima can appear during the optimization.

The other approach to aerodynamic design is the inverse method, where the pressure distribution is specified and the analysis determines the required geometry. Inverse methods are generally much cheaper to use than optimization methods, although optimum designs do not arise directly. Inverse methods also require that the user appreciate several aerodynamic subtleties, the most fundamental being the possibility of specifying a pressure distribution for which a geometry does not exist! The problems of physically unrealistic geometries, existence of solutions, and body closure have been extensively investigated by Volpe and Melnik[4,5] and Volpe[6] for transonic speeds. The selection of the actual target pressure distribution, which is directly related to the body closure problem, must be based on previous design experience. Generally, this amounts to selecting a pressure distribution that controls adverse viscous effects and, especially in the supersonic case, minimizes drag.

Numerous inverse design procedures have been developed, but most of the effort has been directed toward flows with subsonic freestream speeds. Less effort has been devoted to the development of inverse methods for supersonic and hypersonic bodies. The most recent work appears to be the methods developed by Lewis and Sirovich[7] and Fong and Sirovich.[8] However, it appears that the approach developed by Davis[9] provides the most fruitful avenue of development. In that approach, the inverse method is developed by using existing analysis methods. The reason for adopting this approach is the large amount of effort expended on analysis methods that can be used directly, together with the general tendency of direct analysis methods to be more robust than inverse methods. The idea of modifying geometry in analysis codes to obtain inverse methods can be traced to the work of Barger and Brooks.[10] More recently, the approach has been used by Campbell and Smith.[11]

In this paper, a new inverse method using the Euler equations is developed for supersonic and moderate hypersonic flow over axisymmetric bodies. The emphasis is placed on obtaining an efficient and robust method throughout a wide range of supersonic and hypersonic speeds. The development process is emphasized, with results of several variations of the concept presented for a wide range of test cases.

For bodies that have very slightly blunted noses, previous work by the authors[12] has demonstrated that space marching can be used even though there exists a detached shock and locally subsonic region just at the nose. The round nose induced subsonic axial flow

Received Jan. 3, 1991; presented as Paper 91-0395 at the AIAA 29th Aerospace Sciences Meeting, Reno, NV, Jan. 7–10, 1991; revision received June 26, 1991; accepted for publication July 23, 1991.

*Graduate Research Assistant, Department of Aerospace and Ocean Engineering; currently Senior Researcher, Agency for Defense Development, Republic of Korea. Member AIAA.

†Associate Professor, Department of Aerospace and Ocean Engineering. Associate Fellow AIAA.

region will occur on a scale much smaller than the aerodynamic design length scale for atmospheric cruise vehicles. Thus we can neglect this region and use a space-marching procedure to minimize computing time when designing for prescribed surface pressure distributions. For cases where this region must be explicitly accounted for, the present method can be used downstream of the embedded subsonic region.

Description of the Method

General Approach

Following Davis,[9] we use an existing analysis method as the basis for the inverse procedure. Minimum modifications are made to the code, and we plan the modifications for easy implementation in new analysis methods as they become available. For the computations presented here we use the code known as cfl3de, which employs the numerical procedure described by Thomas et al.[13] to solve the Euler or thin-layer Navier-Stokes equations using either an equilibrium air model or a perfect gas model. The code is capable of handling general three-dimensional subsonic, supersonic, and hypersonic flows, although the current inverse method is applied to axisymmetric bodies at zero angle of attack. This allows the method to be developed with a minimum of computational expense. The cfl3de code provides for space-marching solutions to be obtained when appropriate. The inverse method presented in this paper is directed toward design at supersonic and hypersonic speeds, and the space-marching option of cfl3de is used for economy in integrating the Euler equations.

The new inverse method steps one grid plane at a time, using the same approach at each station. One initial plane of data, including pressure and geometry, is required to start the calculation. Then, at each successive station downstream the body geometry required to obtain the prescribed pressure coefficient is determined. The key idea is the use of an approximate algebraic surface pressure-body shape rule to change the shape from an initial estimate to the value required to obtain the desired target pressure distribution. Because there is no exact algebraic relation between the local slope change and pressure change, this is an iterative procedure. As with essentially all nonlinear iteration procedures, convergence is not guaranteed, and a robust numerical approach has been developed tailored to the physics of the problem to produce a reliable design tool. The mechanics of the process are as follows.

Given the initial pressure P_i, the local Mach number M_L at the ith plane is calculated from the point isentropic relations. This local Mach number is then used in a local application of a surface pressure-body shape rule.

During the iterations within the inverse routine, M_L is updated with the calculated pressure (M_L can be fixed during the inverse iterations but convergence is worse). Using one of the surface pressure-geometry relations described in the next section, the geometry at iteration k is obtained from the calculated pressure P_i and local Mach M_L number using the equation

$$\left(\frac{\mathrm{d}z}{\mathrm{d}x}\right)^k = \left(\frac{\mathrm{d}z}{\mathrm{d}x}\right)^{k-1} + \frac{\mathrm{d}}{\mathrm{d}C_p}\left(\frac{\mathrm{d}z}{\mathrm{d}x}\right)^{k-1}\left[C_p^T(i) - C_p^{k-1}(i)\right] \quad (1)$$

The pressure and body slope are computed here at the center of the cell, station $i - 1/2$, consistent with the finite volume numerical scheme. The body shape at station i is then constructed assuming a constant slope between the i and $i-1$ computational stations. The body slope is second order accurate since it is found from a central difference. The resulting shape is formally first order accurate.

The new grid system is generated next from the new geometry, and the computation is performed with this new geometry. The inverse iteration procedure proceeds until the difference of the calculated pressure and target pressure is within some prescribed tolerance. In most cases a convergence criterion δ of order 10^{-4} is acceptable, i.e.,

$$\left|C_p^{(k)}(i) - C_p^T(i)\right| \le \delta \quad (2)$$

In subsonic and transonic inverse methods previously developed,[4,5,11] a starting body shape was required to start the inverse calculation. By using space marching for supersonic and hypersonic flow calculations, a starting body shape is not required. In each marching plane, the body shape is determined from the initial surface pressure using one of the pressure-shape rules. Moreover, we are not concerned with the existence of the resulting body a priori because the body shape is found in each marching plane, and the solution can simply be halted automatically if the specified pressure distribution leads to a body that would require a negative radius according to the calculation. This is a significant advantage in the present space-marching inverse Euler method.

Surface Pressure and Body Geometry Relations

Many approximations relating the surface pressure to the body geometry can be identified. Among these, approximations that are relatively easy to apply and appropriate to the speed range have been considered as candidates for the axisymmetric inverse calculation procedure. The four most important surface pressure-body geometry rules that were considered are the following:

Linearized supersonic theory[14]:

$$C_p = \frac{2}{\sqrt{M_\infty^2 - 1}} \tan\theta \quad (3)$$

Two-dimensional shock-expansion formula that is valid from supersonic to moderate hypersonic flow[15]:

$$C_p = \frac{2}{M_\infty} m\sin\theta + \frac{\gamma+1}{2}(m\sin\theta)^2 + \left(\frac{\gamma+1}{4}\right)^2 M_\infty (m\sin\theta)^3 \quad (4)$$

where

$$m^2 = \frac{M_\infty^2}{M_\infty^2 - 1} \quad (5)$$

Tangent-cone approximation in hypersonic flow[16]:

$$C_p = \tau\frac{k_1^2}{M_\infty^2}\left(1 + \frac{1}{5\gamma k_1^{3/2}}\right) \quad (6)$$

where

$$k_1 = M_\infty\theta \quad (7)$$

$$\tau = 2(\gamma+1)(\gamma+7)/(\gamma+3)^2 \quad (8)$$

Newton impact theory[17]:

$$C_p = 2\sin^2\theta \quad (9)$$

Using these pressure-body geometry rules, we apply the inverse routine to example calculations and identify the most promising pressure-body geometry rule, that is, the one that has the most robust convergence behavior and least computation time. In the process a standard numerical method, which appears to be unique in its application to inverse calculations, will be demonstrated and compared with the other methods. To use the rules given previously, a different form is required. Define a coefficient $A(M_L, \theta)$ relating the surface pressure change to the body geometry change for each pressure-geometry rule. This coefficient should properly reflect the change of the surface pressure on the corresponding change of the body geometry at the design Mach number. Otherwise, during the numerical iteration procedure the resulting body geometry oscillates or diverges. The rules given previously result in a wide range of values for the coefficient. Convergence depends on the numerical value of this coefficient, which is a function of the local Mach number and the body shape. Henceforth, we identify Eqs. (3), (4), (6), and (9) as the linearized supersonic, shock-expansion, tangent-cone, and Newtonian pressure-shape rules, respectively.

The surface pressure-body shape rules given earlier can be equivalently expressed in the form required to implement the method by finding the change in pressure due to a change in body slope. The form of the rules can then be expressed as

$$\Delta C_p = A(M_L, \theta)\,\Delta\theta \quad (10)$$

where ΔC_p is $C_p^T - C_p^{k-1}(i)$ and $\Delta\theta$ is $\tan^{-1}(dz/dx)^k \tan^{-1}(dz/dx)^{k-1}$, for use as given in Eq. (1). Following Ref. 9, we take M_∞ as the local Mach number M_L. This interpretation was adopted due to the success of Davis[9] at transonic and low supersonic speeds. The idea is to make local geometry changes based on local flow conditions. The actual value of A is somewhat insensitive to the use of either M_∞ or M_L. At $M_\infty = 6$ the values are nearly identical for the shock-expansion formula and at the high Mach number limit the Newtonian rule is valid and is independent of Mach number. As stated earlier, convergence was improved when the M_L was updated during the iteration. $A(M_L,\theta)$ is defined as the change of surface pressure with respect to the change of body slope angle. This is determined by the surface pressure-body shape rules given earlier in Eqs. (3–9). The pressure-geometry rules become

Linearized supersonic pressure-shape rule:

$$A(M_L,\theta) = \frac{2}{\sqrt{M_L^2-1}}\sec^2\theta \tag{11}$$

Shock-expansion pressure-shape rule:

$$A(M_L,\theta) = m\cos\theta\cdot\left[\frac{2}{M_L} + (\gamma+1)m\sin\theta + \frac{3}{16}(\gamma+1)^2 M_L m^2 \sin^2\theta\right] \tag{12}$$

where

$$m^2 = \frac{M_L^2}{M_L^2-1} \tag{13}$$

Tangent-cone pressure-shape rule:

$$A(M_L,\theta) = \tau(2\theta + 1/2c\theta^{-1/2}) \tag{14}$$

where

$$c = (5\gamma M_L^{3/2})^{-1} \tag{15}$$

Newtonian pressure-shape rule:

$$A(M_L,\theta) = 2\sin 2\theta \tag{16}$$

The $A(M_L,\theta)$ is shown as a function of the body surface slope θ in Fig. 1 for Mach 6.0 for each rule. The value of $A(M_L,\theta)$ must be positive because ΔC_p and $\Delta\theta$ must have the same sign for all slopes θ (both compression and expansion).

The value of $A(M_L,\theta)$ for the shock-expansion pressure-shape rule is positive for the entire body slope range and changes properly with θ. Thus, this rule can be applied to any target pressure distribution. It is essentially exact for two-dimensional flow.

The $A(M_L,\theta)$ for the linearized supersonic pressure-shape rule is nearly constant for a wide range of body slope. With the shock expansion result being nearly correct, it is seen that the accuracy of the linearized supersonic rule is poor. Using this rule, either the converged body geometry could not be obtained (oscillating during the inverse iteration for a moderate hypersonic Mach number, say $M_\infty = 6.28$) or took too much time to obtain a converged solution (at supersonic speeds). This pressure-shape rule, which was proposed by Barger and Brooks[10] to apply to the inverse method, is difficult to apply to hypersonic flows without modification because it fails to capture the hypersonic flow physics, resulting in convergence problems.

The tangent-cone and Newtonian pressure-shape rules assume positive surface pressure coefficients, and thus these rules have convergence problems for regions of negative pressure coefficient specification. The value of $A(M_L,\theta)$ in these rules is negative for the negative body slope region as can be seen in Fig. 1, and a converged body shape cannot be obtained with negative values of $A(M_L,\theta)$ as described earlier. This means that these rules cannot be applied to the regions of negative pressure coefficient specification. Moreover, the value of $A(M_L,\theta)$ for the tangent-cone pressure-shape rule becomes very large (infinite for the particular approximation used here) as the body slope vanishes. This means that we cannot obtain a converged body shape from the given pressure specification in negative or zero body slope regions.

For a specific application, the rule that most closely captures the physics should be used. Texts such as Carafoli[15] and Cox and Crabtree[17] review the relative accuracy and regions of application. Tables demonstrating the relative performance of the various rules are presented later.

Adaptation to Incorporate Root-Finding Scheme

The convergence issues discussed previously can be resolved by treating the iteration for the body shape corresponding to the prescribed pressure at a particular station as a root-finding problem. This procedure will be illustrated in the next section.

Based on initial results using the method, an alternate scheme was adopted. Mathematically, the objective of the inverse method is to find the body geometry that will make the difference between the pressure at the current iteration and the target pressure zero. Thus, the inverse routine can be interpreted to be a root-finding scheme between ΔC_p and body slope (the body geometry is updated during the inverse iterations to drive ΔC_p to zero). The Regula-Falsi root-finding scheme[18] (a bracketing root-finding method that is very robust) was incorporated into the inverse method. At least two inverse iterations using Eq. (10) are needed to bracket the root and start the Regula-Falsi scheme. The number of root-finding iterations required depends on how close the initial results are to the actual solution. Thus, the convergence behavior depends on which pressure-shape rule is used to start the root-finding scheme. After its introduction for the test cases with negative body slope angle, in which converged body geometries could not be obtained, it was adopted as part of the general method. The result of introducing the Regula-Falsi scheme into the method will be illustrated in the results section. Although a method more efficient than Regula-Falsi could be used, most results were obtained with such a low iteration count that little advantage could be found for adopting another root-finding method.

Numerical Evaluation for Axisymmetric Bodies

The inverse routine and pressure-shape rules, which were developed and explained in the previous sections, are now applied to supersonic and hypersonic axisymmetric body test cases. Inverse calculations were performed for six different target pressure distributions in the supersonic and moderate hypersonic speed range. Four approximations of the surface pressure to the body shape and supersonic and hypersonic Mach number effects are investigated for each case. Using this information, the method that has the fast-

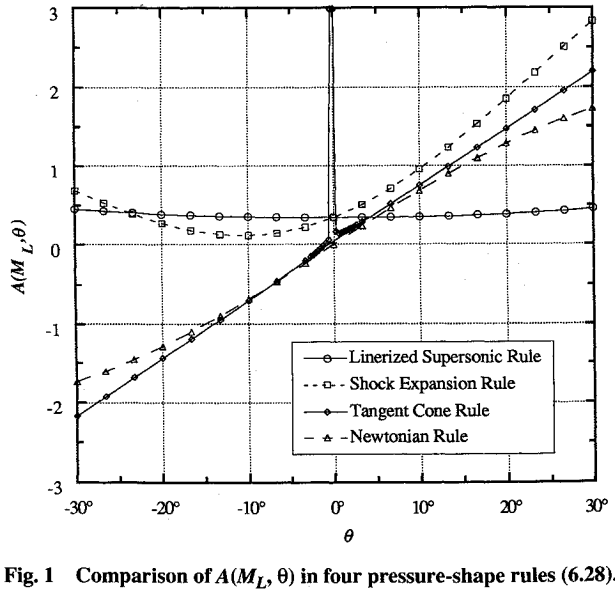

Fig. 1 Comparison of $A(M_L,\theta)$ in four pressure-shape rules (6.28).

est convergence and demonstrates the most robust behavior was identified.

For these calculations, 41 stations were used along the body, with stations clustered near the nose. Between the body and outer edge of the grid 20 points were used, with clustering near the body. Previous numerical experiments[12] demonstrated that this grid resolution was sufficient to obtain accurate results for analysis cases of the general class considered here.

The axial computational grid at $M_\infty = 6.28$ is shown in Fig. 2a for the nominal body (3/4 power law shape). Figures 2b and 2c illustrate the grid arising for two inverse calculations. Using this grid system, computations were made on the Virginia Polytechnic Institute and State University IBM 3090 computer. Typical CPU time for the first 10% of the length from the nose (marching planes $i = 1 \sim 13$) is 3 min. It takes 53 s to compute the flow over the rest of the body (from $i = 14 \sim 41$) in the analysis calculation. The CPU time for inverse calculations is heavily dependent on the pressure-shape rules and will be examined in detail later.

Hypersonic Minimum Drag Body (Power Law Shape)

To validate the inverse calculation routine developed for axisymmetric supersonic and hypersonic bodies, sample calculations were performed for the 3/4 power law shape previously studied.[12] For freestream Mach numbers 3.0 and 6.28, the results showed that the known body geometry could be found typically within three inverse iterations at each marching station by using the tangent-cone pressure-shape rule.

Test Cases

Four test case target pressure distributions have been selected. The target pressure coefficient distributions are shown together with the resulting body shape solutions in Figs. 3–6. Each one is discussed next.

Test Cases I and II

Test target pressures I & II are selected to demonstrate the capability to obtain the body geometry for negative pressure coefficient distributions (including pressures near vacuum: C_{pvac} is -0.036 for $M_\infty = 6.28$). The two target pressure distributions are prescribed as follows:

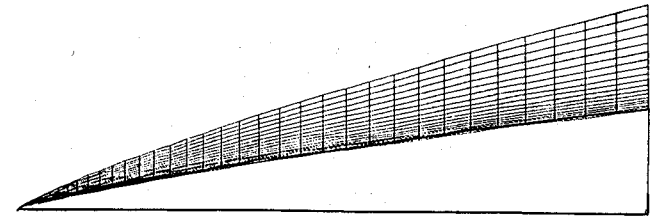

(a) Nominal Body (3/4 Power Law Shape)

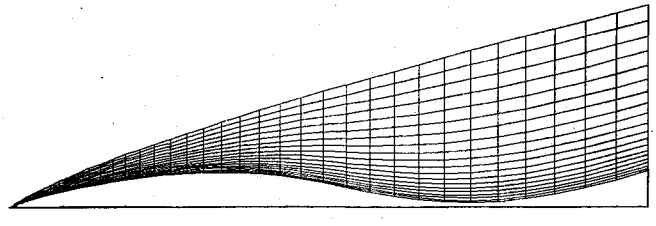

(b) Test Case I

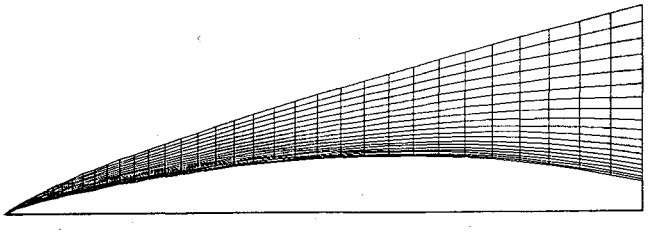

(c) Test Case II

Fig. 2 Axial computational grids for axisymmetric inverse test cases.

Test case I: Pressure is minimum (near C_{pvac}) at 50% of the body length from the nose and then increases quadratically to the end of the body.

Test case II: Specified pressure decreases continuously from the starting point of the inverse option to the end of the body where the pressure is minimum (near C_{pvac} for $M_\infty = 6.28$).

As mentioned in the previous section, using the linearized supersonic pressure-shape rule, a converged body geometry cannot be obtained from the given target pressure for $M_\infty = 6.28$ (hypersonic flow), but for $M_\infty = 3.0$, the value of $A(M_L, \theta)$ is larger than that for $M_\infty = 6.28$ and is large enough to get a converged solution. However, this pressure-shape rule requires relatively long computation times to obtain a converged solution. Typically, the CPU time is $5 \sim 6$ times longer than that of the direct calculation and the number of inverse iterations in each marching plane is $2 \sim 7$. These findings are summarized in Table 1. Since this pressure-shape rule comes from the linearized supersonic theory approximation, it is not surprising that it does not work for higher Mach numbers (in this case, $M_\infty = 6.28$).

Based on this initial experience, the variation in the scheme was adopted using the linearized supersonic pressure-shape rule. The effect of introducing the Regula-Falsi root-finding scheme is clearly shown in Table 1. Using this method, we get a converged geometry for the given surface pressure distributions. For $M_\infty = 6.28$, we can get a converged geometry, and, moreover, we can get an improved convergence for $M_\infty = 3.0$ (approximately 1.2 times faster for test cases I and II). It also requires a smaller number of inverse iterations in each space marching plane than that without Regula-Falsi scheme (it has $2 \sim 4$ inverse iterations in each plane).

The shock-expansion pressure-shape rule comes from the shock-expansion theory for supersonic and moderate hypersonic flow. Thus, it is applicable to regions of negative body slope and negative pressure coefficient distributions. Eggers and Savin[19] noted that hypersonic flow over three-dimensional bodies can be approximated as locally two dimensional, and hence two-dimensional shock-expansion theory is a valid approximation. In other words, this approximation, in nature, has wide applications [this can be expected from the fact that the value of $A(M_L, \theta)$ is greater than zero for all body slopes θ, in Fig. 1]. As can be seen in Table 1, converged solutions were obtained for all of the test cases. The only problem is that it requires relatively high computation time and a larger number of inverse iterations in each marching plane. Typical CPU time is $5 \sim 7$ times longer than that of the direct calculation for test case I and $4 \sim 6$ times longer for test case II, and the number of inverse iterations in each marching plane is $2 \sim 11$ for test case I, $2 \sim 6$ for test case II. With the application of the Regula-Falsi root-finding scheme, as found in the linearized supersonic pressure-shape rule, CPU time is greatly reduced ($1.2 \sim 1.5$ times faster for test cases I and II).

Because of the negative pressure coefficient regions in test cases I and II, the resulting body geometry will have negative and zero slopes at some stations. As shown in the previous section, the tangent-cone and Newtonian pressure-shape rules have difficulties near zero and negative body slope. The value of $A(M_L, \theta)$ becomes very large for the tangent-cone rule, and it goes to zero in the Newtonian rule near zero slope. Neither of these situations is suitable for inverse calculation. Furthermore, the values of $A(M_L, \theta)$ in these rules are negative when the body slope is negative. As mentioned earlier, a converged body geometry cannot be obtained with a negative value of $A(M_L, \theta)$. In an attempt to apply this rule to arbitrary pressure distributions, the first author modified Eqs. (14) and (16) in an ad hoc manner as follows for the tangent-cone and Newtonian pressure shape rules, respectively:

$$A(M_L, \theta) = \tau(2\theta + 1/2c|\theta|^{-1/2}) \tag{17}$$

and

$$A(M_L, \theta) = 2|\sin 2\theta| \tag{18}$$

These modifications were used to bracket the root for use with the Regula-Falsi scheme to get converged solutions for target pressure distributions containing negative pressure coefficient regions. Using the Regula-Falsi scheme, the convergence rate, number of inverse iterations in each marching plane, and total CPU time are greatly improved, as shown in Table 1. The modified tangent-cone rule, Eq. (17), resulted in the fastest convergence and least computation time compared with the other pressure-shape rules considered (about 2.0 ~ 2.9 times longer than that of the direct calculations). A converged solution is obtained within 3 ~ 4 inverse iterations in each marching plane. This is remarkable comparing other inverse codes developed previously, for which more than 10 inverse iterations are typically required.[11]

The computation time for $M_\infty = 6.28$ is slightly less than that for $M_\infty = 3.0$ even though there is no difference in computation time between $M_\infty = 6.28$ and 3.0 for the direct calculation. That is because the tangent-cone pressure-shape rule was derived for hypersonic flow.

The calculated body geometries for the given target pressure distributions are shown in Figs. 3 and 4 for Mach numbers of 3.0 and 6.28. The calculated body for $M_\infty = 6.28$ is more sensitive to the target pressure than that for $M_\infty = 3.0$. This is because the body slope is roughly proportional to local Mach number for the given pressure coefficient.

Test Case III

The test target pressure III decreases slowly to 40% of the body length from the nose and then increases quadratically to the end of the body as shown in Fig. 5. The convergence behavior and number of inverse iterations required to obtain the solution are tabulated in Table 2 for all pressure-shape rules with and without the Regula-Falsi scheme. The calculated body geometries for the given target pressure distribution are shown in Fig. 5 for Mach numbers 3.0 and 6.28. As expected from the positive target pressure coefficients, the body diameter increases from the nose to the end of the body. The abrupt increase of the body thickness in the end region will cause a large drag increase.

Table 1 Convergence behavior of several pressure-shape rules for test case I

Pressure-shape rules	$M = 3.0$ CPU (inverse)/CPU (direct)	$M = 3.0$ No. of iterations	$M = 6.28$ CPU (inverse)/CPU (direct)	$M = 6.28$ No. of iterations
Linearized supersonic	4.08	2–7	No convergence	
Shock-expansion	4.55	2–7	5.74	2–11
Tangent-cone	No convergence		No convergence	
Newtonian	No convergence		No convergence	
Linearized supersonic with Regula-Falsi	3.49	2–4	3.71	3–5
Shock-expansion with Regula-Falsi	3.54	2–5	3.91	2–5
Tangent-cone with Regula-Falsi	2.89	2–4	2.62	1–4

Table 2 Convergence behavior of several pressure-shape rules for test case III

Pressure-shape rules	$M = 3.0$ CPU (inverse)/CPU (direct)	$M = 3.0$ No. of iterations	$M = 6.28$ CPU (inverse)/CPU (direct)	$M = 6.28$ No. of iterations
Linearized supersonic	6.34	6–9	No convergence	
Shock-expansion	5.81	6–7	3.90	3–5
Tangent-cone	2.53	1–3	1.94	1–3
Newtonian	5.92	5–7	3.03	2–5
Linearized supersonic with Regula-Falsi	3.81	4	4.80	4–9
Shock-expansion with Regula-Falsi	4.28	4–5	3.86	3–6
Tangent-cone with Regula-Falsi	2.49	2–4	2.00	2–3

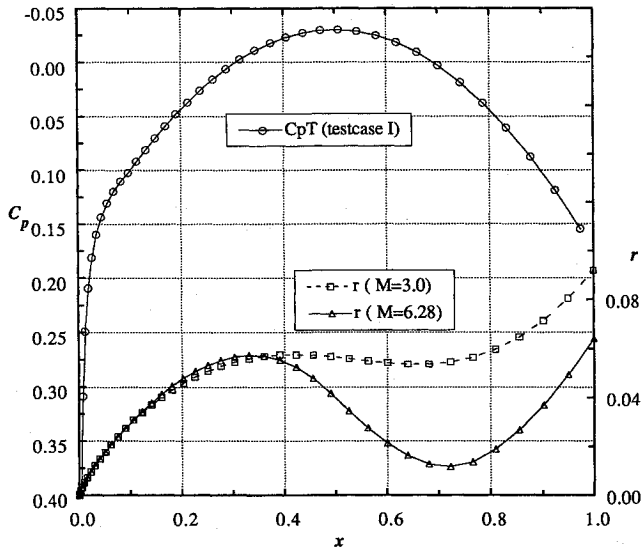

Fig. 3 Test target pressure I and resulting body shape.

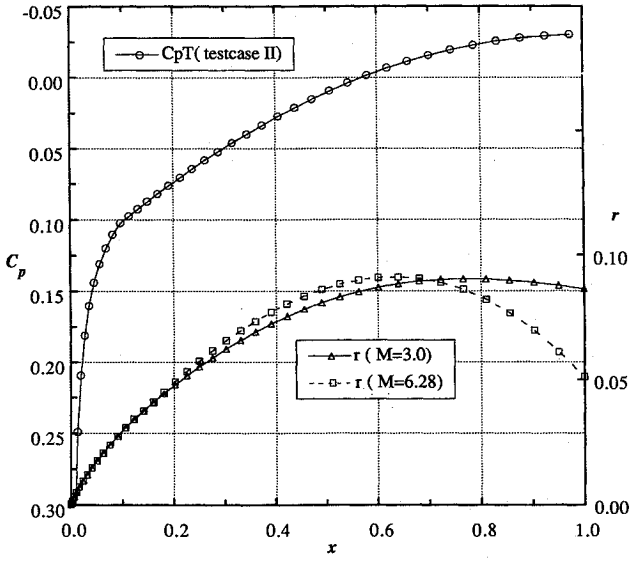

Fig. 4 Test target pressure II and resulting body shape.

Test Case IV

Test case IV is chosen to demonstrate the method's ability to obtain the body geometry resulting from an abrupt change of the surface pressure distribution. The test target pressure coefficient distribution is selected to decrease linearly from the starting plane of the inverse calculation and then is held at zero when that value is reached (30% of the body length from the nose to the end of the body).

The target pressure distribution and the calculated body shape for each Mach number is given in Fig. 6. From this figure, we can see the mild corner in the body geometry in the region where the specified pressure coefficient changes abruptly to zero. Note that the body radius continues to increase even though the pressure

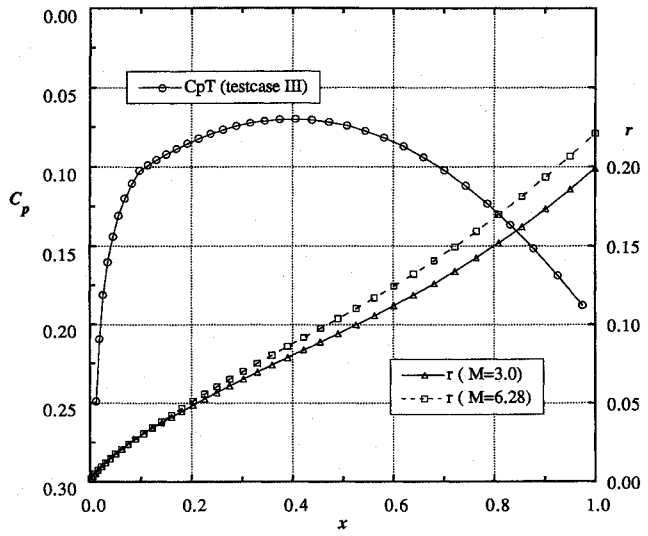

Fig. 5 Test target pressure III and resulting body shape.

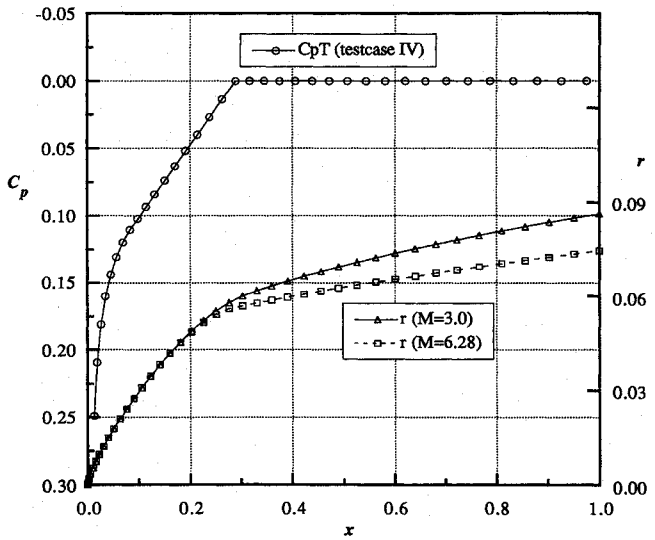

Fig. 6 Test target pressure IV and resulting body shape.

coefficient is zero. This test case shows that the method can handle the case of a target pressure distribution with an abrupt change without difficulty.

The tangent-cone pressure-shape rule with Regula-Falsi scheme is applied for $M_\infty = 3.0$. The number of inverse iterations in each space-marching plane is 1 ~ 4 (maximum number of inverse iterations occurred at the corner) and the total CPU time is 2.3 times longer than that of a direct calculation. The linearized supersonic pressure-shape rule with the Regula-Falsi scheme is applied for $M_\infty = 6.28$. The number of inverse iterations in each space-marching plane is 3 ~ 4 (maximum number of inverse iterations occurred at the corner) and total CPU time is 3.6 times longer than that of direct calculation.

Ogive Cylinder (Body with a Corner, $l/d = 3.0$)

To demonstrate the capability of obtaining a body shape with a corner, the method was tested for a known geometry, the secant-ogive cylinder. The results for this case were obtained without difficulty, exactly duplicating the body shape.

Speed Range of Application

This work has examined the supersonic ($M_\infty = 3.0$) and moderate hypersonic ($M_\infty = 6.28$) speed range typical of atmospheric cruise vehicles. Although not demonstrated at higher speed, application to higher speeds appears to be straightforward for bodies with positive target pressure coefficient distributions. Results presented in Table 2 showed that the tangent-cone rule worked much better with increasing speed for that class of pressure distribution.

Conclusions

An efficient inverse method has been presented for supersonic and moderate hypersonic axisymmetric body design. Numerous surface pressure-body geometry rules have been compared and the most robust and fastest rule suitable for inverse calculations has been identified: the modified tangent-cone Regula-Falsi scheme. A new method to accelerate the convergence rate during the inverse iterations was proposed and run successfully for many example calculations: CPU times are approximately twice direct analysis times. Numerous examples in both supersonic and moderate hypersonic flow were presented to demonstrate the robustness of the method. Although the method has been developed and demonstrated for the case of axisymmetric flow, the analysis provides the foundation for a general three-dimensional inverse design method for the supersonic and hypersonic flow regimes.

Acknowledgments

We would like to acknowledge R. W. Walters of Virginia Polytechnic Institute and State University for providing us with access to cfl3de. The computer resources required to develop the method were provided by the Department of Aerospace and Ocean Engineering at Virginia Polytechnic Institute and State University.

References

[1]Harris, R. V., Jr., "On the Threshold—The Outlook for Supersonic and Hypersonic Aircraft," 52nd AIAA Wright Brothers Lecture, AIAA Paper 89-2071, Aug. 1989.

[2]Powell, A. G., Agrawal, S., and Lacey, T. R., "Feasibility and Benefits of Laminar Flow Control in Supersonic Cruise Airplanes," NASA CR-181817, July 1989.

[3]Aidala, P. V., Davis, W. H., Jr., and Mason, W. H.,"Smart Aerodynamic Optimization," AIAA Paper 83-1863, July 1983.

[4]Volpe, G., and Melnik, R. E., "The Design of Transonic Aerofoils by a Well-Posed Inverse Method," *International Journal for Numerical Methods in Engineering*, Vol. 22, No. 2, 1986, pp. 341–361.

[5]Volpe, G., and Melnik, R. E., "The Role of Constraints in the Inverse Design Problem for Transonic Airfoils," AIAA Paper 81-1233, June 1981.

[6]Volpe, G.,"The Inverse Design of Closed Airfoils in Transonic Flow," AIAA Paper 83-0504, Jan. 1983.

[7]Lewis, T. S., and Sirovich, L., "The Inverse Problem for Supersonic Airfoils," *AIAA Journal*, Vol. 22, No. 2, 1984, pp. 295–297.

[8]Fong, J., and Sirovich, L., "Direct and Inverse Problem in Supersonic Axisymmetric Flow," *AIAA Journal*, Vol. 24, No. 5, 1986, pp. 852–854.

[9]Davis, W. H., Jr., "Technique for Developing Design Tools from the Analysis Methods of Computational Aerodynamics," *AIAA Journal*, Vol. 18, No. 9, 1980, pp. 1080–1087.

[10]Barger, R. L., and Brooks, C. W., Jr., "A Streamline Curvature Method for Design of Supercritical and Subcritical Airfoils," NASA TN D-7770, Sept. 1974.

[11]Campbell, R. L., and Smith, L. A., "A Hybrid Algorithm for Transonic Airfoil and Wing Design," AIAA Paper 87-2552, Aug. 1987.

[12]Mason, W. H., and Lee, J., "On Optimal Supersonic/Hypersonic Bodies," AIAA Paper 90-3072, Aug. 1990.

[13]Thomas, J. L., van Leer, B., and Walters, R. W., "Implicit Flux-Split Schemes for the Euler Equations," AIAA Paper 85-1680, July 1985.

[14]Liepmann, H. W., and Roshko, A., *Elements of Gas Dynamics*, Wiley, New York, 1957, pp. 212–215.

[15]Carafoli, E., *Wing Theory in Supersonic Flow*, Pergamon, Oxford, England, UK, 1969, pp. 463–473.

[16]Krasnov, N. F., *Aerodynamics of Bodies of Revolution*, Elsevier, New York, 1970, pp. 463–470.

[17]Cox, R. N., and Crabtree, L. F., *Elements of Hypersonic Aerodynamics*, Academic, New York, 1965, pp. 97–100.

[18]Gerald, C. F., and Wheatley, P. O., *Applied Numerical Analysis*, 3rd ed., Addison-Wesley, Reading, MA, 1984, pp. 8–10.

[19]Eggers, A. J., Jr., and Savin, R. C., "A Unified Two-Dimensional Approach to the Calculation of Three-Dimensional Hypersonic Flows, with Application to the Bodies of Revolution," NACA Rept. 1249, Aug. 1952.